Calculation Methodology for Effective Bundle-Average Fuel Temperature Correlation©

T. Liang, M. Dahmani and R. McArthur
Candu Energy Inc., Mississauga, Ontario, Canada
(tony.liang@candu.com, mohamed.dahmani@candu.com, randall.mcarthur@candu.com)

Abstract

The effective bundle average fuel temperatures are required by the full core reactor physics code RFSP for local parameter calculations to account for the fuel temperature reactivity feedback. For a fuel bundle at specific power and burnup, the neutron multiplication value calculated by the lattice physics code WIMS-AECL with a uniform fuel temperature should be the same as when fuel-pin temperature differences are considered. This methodology is illustrated by deriving the effective bundle average fuel temperature correlations for an example fuel designfor RFSP calculations.

1. Introduction

The effective bundle-average fuel temperature (EBAFT) correlations are required by the full-core reactor physics code RFSP [1] for local-parameter calculations. The correlation is used to calculate the EBAFT as a function of bundle power at different bundle burnups. To derive the correlation, WIMS-AECL [2] is used to find the temperature through a reactivity search. This is achieved in such a way that the neutron multiplication value calculated by WIMS-AECL for a bundle at a given specific power and with a uniformly distributed EBAFT, is kept the same as the one calculated with a burnup-dependent fuel temperature for each pin.

Candu Energy Inc. has the capability to prepare the EBAFT correlation for a broad range of fuel types. The present work demonstrates the methodology using ACR-1000 reference fuel.

2. Fuel Description

The ACR-1000®[3] reactor design is described in Reference [3]. ACR reference fuel is similar to CANFLEX®[4] fuel in that they both have 43 pins. However, the centre pin of ACR reference fuel consists of one element of a larger outer diameter whereas the outer three rings consist of 42 elements with a smaller outer diameter.

The central element contains sintered cylindrical pellets of burnable thermal-neutron absorbers used to limit reactivity in the core. The composition of the central element has been optimized to

[3] ACR-1000® (Advanced CANDU Reactor®) is a registered trademark of Atomic Energy of Canada Limited (AECL), used under exclusive license by Candu Energy Inc.

[4] CANFLEX®(CANdu FLEXible fueling) is a registered trademark of Atomic Energy of Canada Limited (AECL) and the Korea Atomic Energy Research Institute (KAERI), used under exclusive license by Candu Energy Inc.

reducethe coolant void reactivity by using a mixture of both dysprosium and gadolinium in a yttrium-stabilized zirconia matrix.

The remaining 42 fuel elements contain sintered cylindrical pellets of low-enriched uranium dioxide (LEU) in a Zircaloy-4 sheath. These LEU fuel elements have an enrichment of 2.4 wt% U^{235}. A small amount gadolinium is blended into the LEU elements (about 1g of Gd per bundle) to suppress the initial reactivity of the fresh bundles being inserted into the reactor and limit the fuelling ripple in the core.

3. Methodology

The calculation was done such that the WIMS-AECL-calculated infinite multiplication factor (k_∞) is the same with distributed fuel temperature (four rings with four different temperatures) as with a uniform temperature (EBAFT). The power history implemented in the WIMS-AECL calculations was taken from an RFSP time-average calculation. The fuel temperature in each pin was calculated using the fuel code ELESTRES[4].

The ELESTRES calculations provide pin-volume-average fuel temperature as a function of fuel element linear power for various pin burnups, for each pin of a fuel bundle.

The fuel-bundle neutron multiplication constant (k_∞) obtained from the WIMS-AECL calculation for distributed fuel temperatures for each of three fuel rings is set as the target k_∞. At each burnup step, the volume average fuel temperature is calculated for the fuel bundle as the first guess of EBAFT in WIMS-AECL calculation. WIMS-AECL calculations provide the relationship between k_∞ and the uniform bundle fuel temperature at given bundle powers and burnups. A correction to the uniform fuel temperature (to get EBAFT) is typically needed to achieve the same infinite multiplication factor (k_∞) as the case of distributed fuel temperature. Based on this information, the correlation between the EBAFT and bundle power is derived.

4. Power History

4.1 Bundle Power History

From an RFSP time-average calculation, the values of bundle burnup for beginning-of-cycle (of refuelling) and end-of-cycle (of refuelling) can be obtained for every bundle in the core. For each bundle, the averaged bundle power is maintained between the beginning-of-cycle and the end-of-cycle. There are 6240 fuel bundles in total in the reactor core, and 6240 × 2 burnups/power points as shown in Figure 1. Two bundle power/burnup histories are generated as distinguished by the use of a 2-bundle shift: one is the average history representing bundles in position 1, 3, 5, 7, 9, 11; the other representing bundles in position 2, 4, 6, 8, 10, 12.

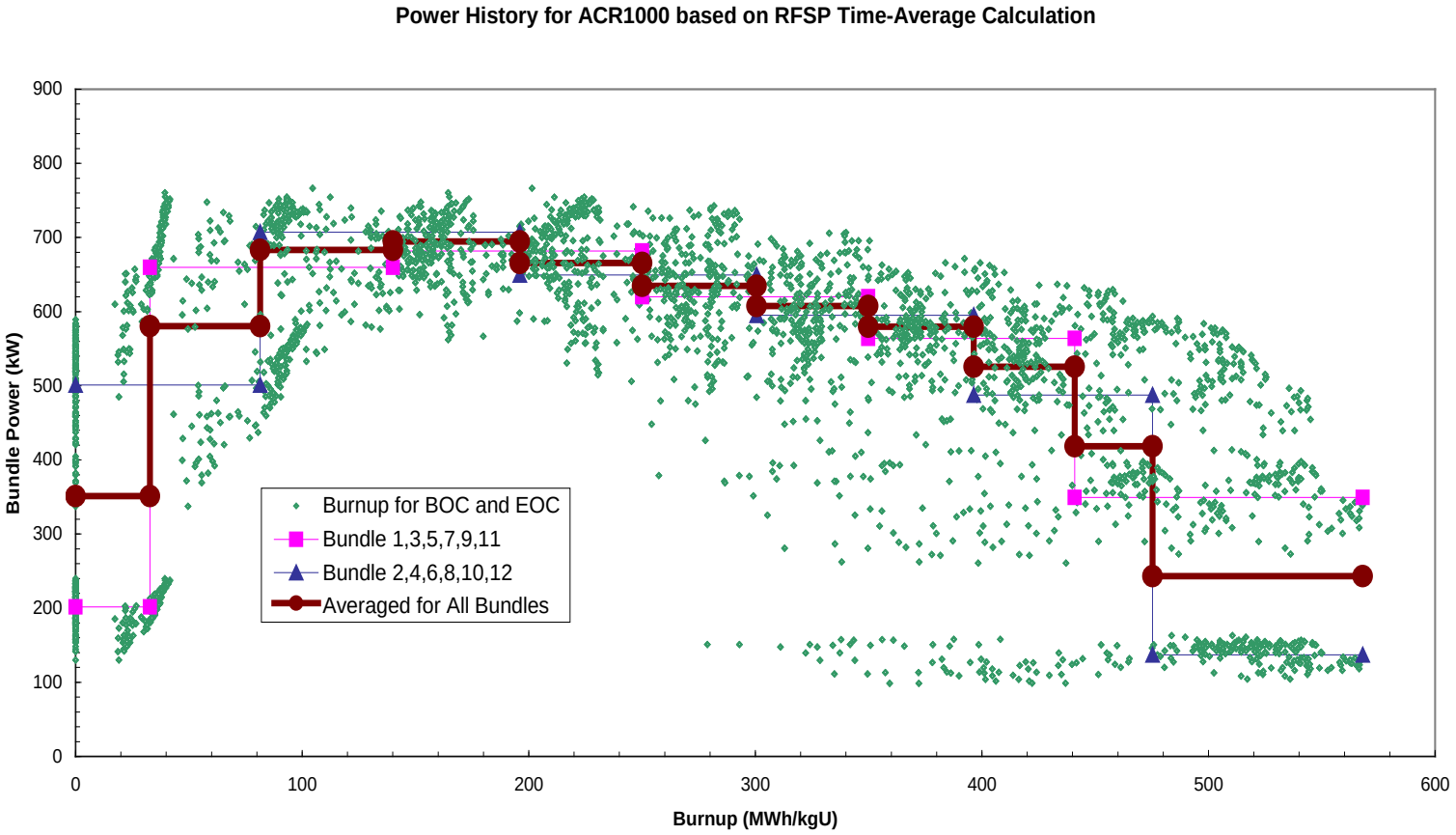

Figure 1 Bundle Power History

(Source: Atomic Energy of Canada Limited. Exclusively licensed to Candu Energy Inc. All rights reserved)

4.2 Pin Power History

The WIMS-AECL model is subdivided into 4 radial annuli and 2 sectors for each annulus. Thus there are 8 semi-annular regions in the fuel pins in each ring. These semi-annuli are shown and referred to as "sectors", in Figure 2.

The following equations were used to convert total bundle linear power to pin linear power, excluding the centre pin since it does not generate power:

$$A = \sum_{i=2}^{4} A_i \tag{1}$$

where,

A is the total cross sectional area of fuel bundle excluding centre pin,cm^2,
A_i is the total cross sectional area of each ring of the fuel bundle, excluding centre pin, i = 2, 3, 4,cm^2.

$$A_i = N_i \sum_{j=1}^{m} A_{ij} \tag{2}$$

where,

m is the total number of sectors in ring i, 8 in total,
A_{ij} is the area of each sector in ring i, The sum of sectors 1 and 2 occupy half of the total area, while the other half is shared by the remaining sectors 3 to 8 equally,cm^2, and
N_i is the number of pins in each ring of the fuel bundle: 7, 14, 21 for Ring 2, Ring 3, and Ring 4, respectively.

$$D_{Ave} = \frac{P}{A} \tag{3}$$

where,

$D_{Ave}$is the average power density, W/cm^3,
P is the total bundle linear power, input in WIMS-AECL, W/cm

$$P_{ij} = r_{ij} D_{Ave} \frac{A_{ij}}{10} \tag{4}$$

where,

P_{ij} is the linear power for each sector, kW/m,
r_{ij} is the relative power density for each sector, dimensionless, output by WIMS-AECL,
10 is the unit conversion coefficient between kW/m and W/cm.

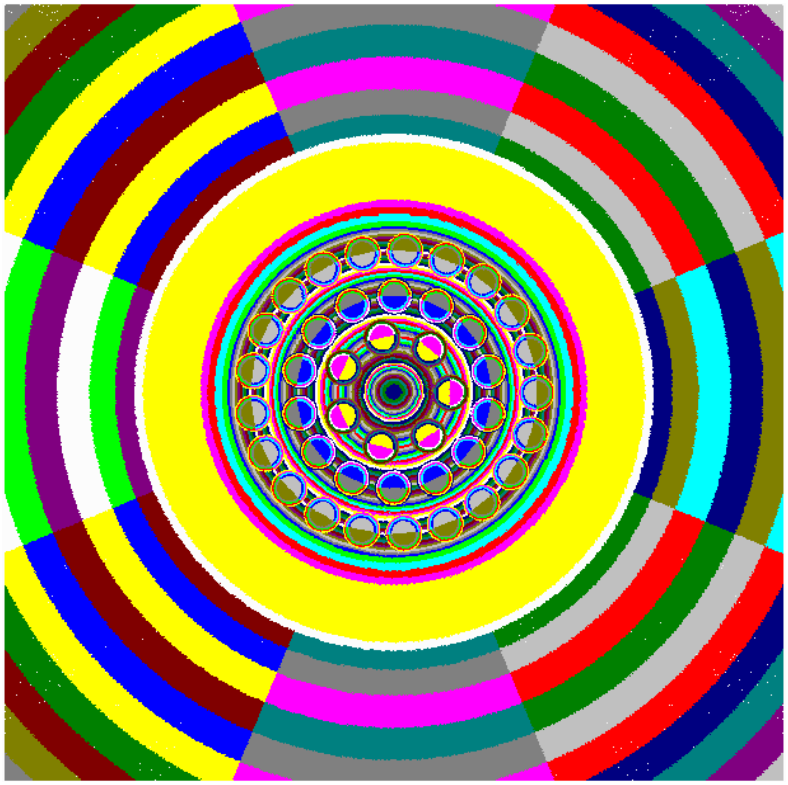

Figure 2 Diagram for WIMS-AECL Calculation Meshes

$$P_i = \sum_{j=1}^{m} P_{ij} \tag{5}$$

where,

P_i is the linear pin power for each ring, kW/m,
P_{ij} is the linear power for each sector, kW/m, and
m is the total number of sectors in ring i, 8 in total.

Pin burnup and pin power were different from ring to ring. WIMS-AECL calculated the powers and burnups for each sector inside each ring. The burnup for each ring was then calculated as the volume average-burnup, considering each sector inside each ring. A small FORTRAN program was used to derive the average power density inside each ring.

Different fuel lengths were used to get the linear powers to be used in WIMS-AECL and in ELESTRES. The fuel bundle length is 49.53 cm, while the fuel stack length is 47.7 cm. For WIMS-AECL, the full fuel length was used to reflect the bundle power in the two dimensional (2D) neutronic transport code. End-region materials were smeared in this 2D model. However, for ELESTRES to calculate a realistic fuel temperature at the pin level, the fuel stack length was used to reflect the linear power of a pin.

Figure 3 shows the pin power-burnup history for each of the three rings that produce power.

5. Fuel-Pin Temperature

The pin power-burnup history was obtained at normal operation (100% full power). The fuel temperature-power correlation differs as the burnup changes because the fuel material composition changes, even though the fuel temperature is determined mainly by the power. To account for the impact of the material composition change on fuel temperature, the fuel temperature was calculated at different burnup steps.

There was a sharp decrease in heat transfer coefficient at the first step caused by densification that is due to irradiation by in-reactor sintering of the UO_2 pellet. Densification results in fuel volume reduction by making the fuel pellet less porous. This in turn could lead to an increase in the radial gap between the pellet and the sheath that affects the heat transfer, and which increases the pellet temperature and the fission gas release. This characteristic of the fuel pin temperature as a function of burnup was included in the analysis.

For each burnup step, there are 13 power levels implemented, which were 1 %, 10 %, 20 %, 30 %, 40 %, 50 %, 60 %, 70 %, 80 %, 90 %, 100 %, 110 %, and 120 % of the “nominal” power, 1000 kW/bundle. A small FORTRAN utility was used to prepare these input files. Figure 4 gives the fuel temperature profile at 0 MWd/teU burnup step. Similar fuel temperature profiles were also produced for other burnup steps.

6. Effective Bundle-Average Fuel Temperature (EBAFT)

Temperatures of rings 2, 3, and 4 were calculated and used in the WIMS-AECL input file at the different burnup steps. The material library from a reference WIMS-AECL run was used to represent the fuel compositions at various burnup steps. For this round of execution of WIMS-AECL, the burnup steps were reflected in the material library.

Using the temperatures of ring 2, 3, and 4, WIMS-AECL calculated the neutron multiplication value at each burnup step corresponding to a specific material library. For the first guess of the EBAFT, a pure volumetric averaged temperature was used and another neutron multiplication value was obtained. This value was compared with the first neutron multiplication value. Typically, these two values should be close to each other. The reactivity differences are a linear function of bundle power level. The maximum difference is about 0.2 mk as shown in Figure 5, an example for Day 233.

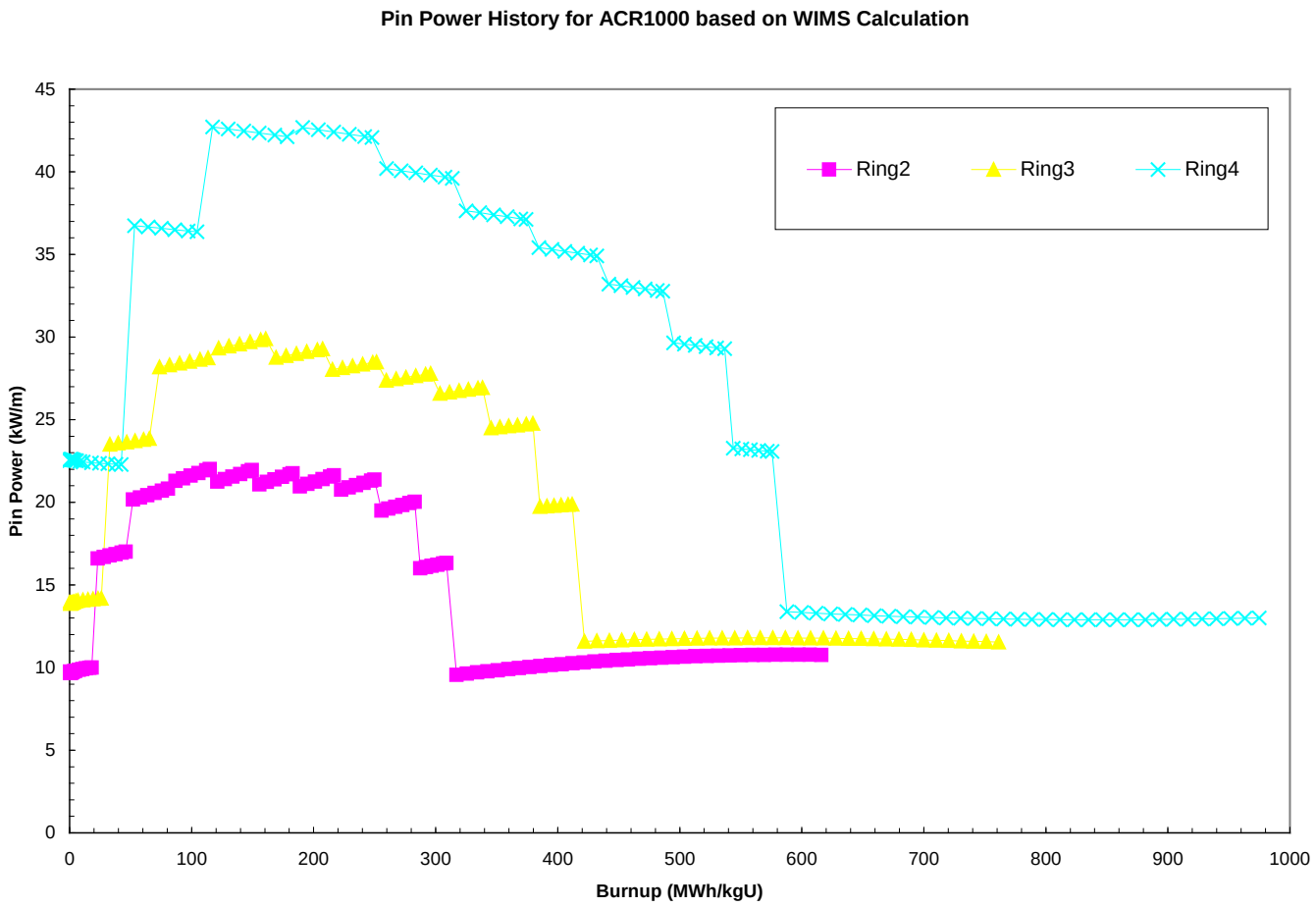

Figure 3 Pin Power History

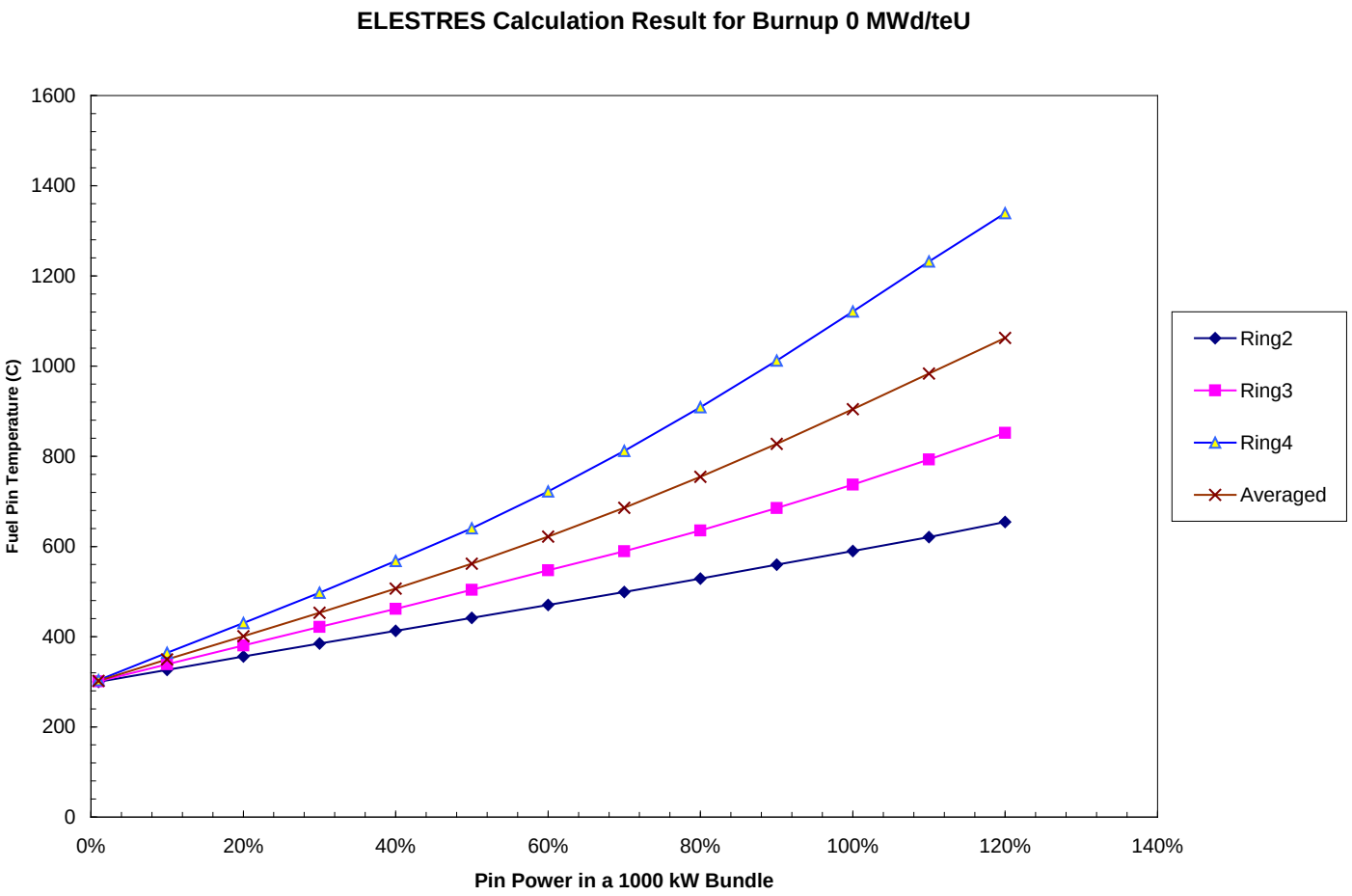

Figure 4. ELESTRES Calculation Result at Burnup 0 MWd/teU

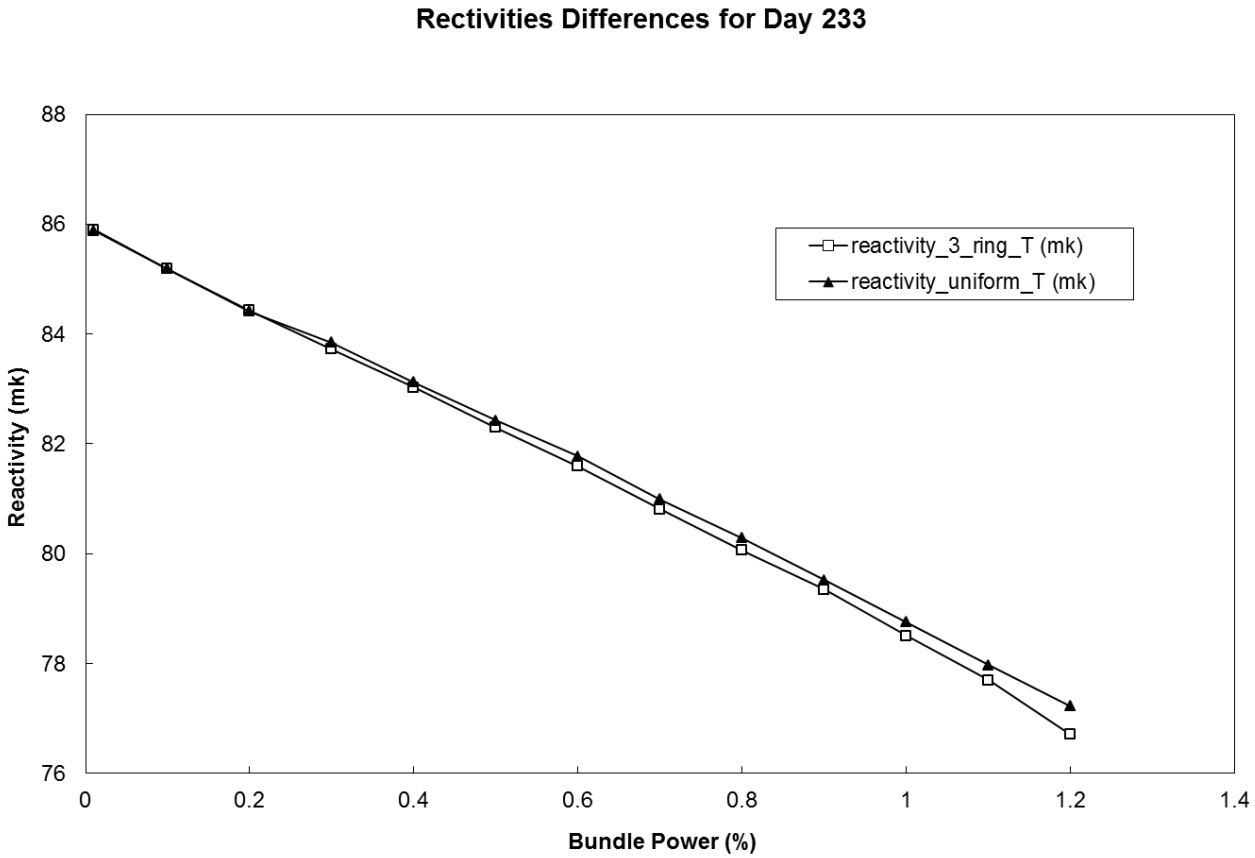

Figure 5. Reactivity Difference between Uniform and Distributed Fuel Temperature Cases

This comparison shows that simply using the volume-averaged temperature to represent the EBAFT is not accurate enough. As such, the EBAFT was modified to achieve the same neutron multiplication value as the cases with radially distributed temperatures. The following modification was made for each volume-averaged fuel temperature to represent the first guess for the EBAFT.

$$T_{eff} = T_{va} + \left(\rho_{tar} - \rho_{va}\right)\frac{T_{va}^{h} - T_{va}^{l}}{\rho_{va}^{h} - \rho_{va}^{l}} \tag{6}$$

$$\text{or} \quad T_{eff} = T_{va} + \frac{\left(\rho_{tar} - \rho_{va}\right)}{\rho_{va}^{h} - \rho_{va}^{l} \Big/ T_{va}^{h} - T_{va}^{l}} = T_{va} + \frac{\left(\rho_{tar} - \rho_{va}\right)}{C_{ft}} \tag{7}$$

where,

T_{eff} is the EBAFT, °C,

T_{va} is the volume-averaged fuel temperature, °C,

ρ_{tar} is the target reactivity, mk,

ρ_{va} is the reactivity at the volume-averaged fuel temperature, mk,

T_{va}^{h} is the volume-averaged fuel temperature at the high-end, which is the fuel temperature of the highest perturbed bundle power case (120 % of nominal power), °C,

T_{va}^{l} is the volume-averaged fuel temperature at the low-end, which is the fuel temperature of the lowest perturbed bundle power case (1 % of nominal power), °C,

ρ_{va}^{h} is the reactivity at the high-end, which is the reactivity of the highest perturbed bundle power case (120 % of nominal power), mk,

ρ_{va}^{l} is the reactivity at the low-end, which is the reactivity of the lowest perturbed bundle power case (1 % of nominal power), mk, and

C_{ft} is the fuel temperature reactivity coefficient, mk/K, it equals to $\rho_{va}^{h}-\rho_{va}^{l} \big/ T_{va}^{h}-T_{va}^{l}$. Its typical value is -0.00014mk/K.

Note that C_{ft} is not a function of temperature, but rather it is an averaged coefficient over a large range of temperatures. The corrected EBAFT is always higher than the volume averaged fuel temperature. The maximum correction to the EBAFT was 53 °C.

7. Derivation of the Correlation of EBAFT verse Bundle Power

A second order polynomial equation was used to derive the correlation as follows.

$$y = ax^2 + bx + c = a \times 0^2 + b \times 0 + c = c \tag{8}$$

where,

y is the EBAFT, °C; and
x is the bundle power, kW/bundle.

To calculate the coefficients in the equation (8), we start by considering an extreme case where the fuel temperature is the same as the coolant temperature when bundle power is zero.

Theoretically, "c" should be equal to coolant temperature. However since the fitting curve is generalized based on a number of scattered points, we would not expect the value of "c" and the coolant temperature to be identical. The correlation could be written in the following format:

$$y = ax^2 + bx + T_c + \Delta T \tag{9}$$

where,

T_c is the coolant Temperature, °C; and
ΔT is the temperature difference, °C.

The coolant temperature used in ELESTRES calculation was 570 K, or 296.84 °C. The correlations were found to be:

$$\begin{aligned} y &= 0.000167639x^2 + 0.472090x + T_c + 6.428 && \left(\begin{array}{l} 0 \le BB \le 359\text{MWd/teU} \\ \text{and } 18373 < BB \le 29694\text{MWd/teU} \end{array}\right) \\ y &= 0.000146837x^2 + 0.458026x + T_c + 6.161 && (359 < BB \le 18373\text{MWd/teU}) \\ y &= 0.000131870x^2 + 0.552888x + T_c + 0.904 && (29694 < BB \le 35088\text{MWd/teU}) \end{aligned} \quad (10)$$

where,

BB is the bundle burnup, MWd/teU.

The power range used in the derivation of these correlations is from 1 % to 120 % of "nominal" power, 1000 kW/bundle. As such, the validity of the correlations can only be guaranteed in this power range. For an accident scenario that goes beyond this range, these correlations may not be valid. For such accident analysis, the fuel temperature will be calculated independently.

The central pin temperature is higher than the coolant temperature because of gamma radiation, but was assumed to be the same temperature as the coolant in this paper. This assumption would have negligible effect on the results.

8. Conclusion

With the code package, RFSP, WIMS-AECL, and ELESTRES, the correlations of EBAFT as a function of bundle power have been derived for different burnup steps.

The methodology applied the power history based on a time-average calculation, and perturbations in power level were applied only at specific burnup steps. The fuel temperature characteristic behaviour at different stages of burnup was considered when selecting the representative burnup steps.

The accuracy of these correlations has been estimated for the demonstration fuel design and it was concluded that they may be used in RFSP for core calculations with that fuel type.

9. Acknowledgements

Some of the information contained in this document is the property of Atomic Energy of Canada Limited and is used under the exclusive license by Candu Energy Inc.

10. References

[1] B. Rouben, "RFSP-IST, the Industry Standard Tool Computer Program for CANDU Reactor Core Design and Analysis", Proceedings of the 13th Pacific Basin Nuclear Conference, Shenzhen, China, 2002 October 21-25.

[2] J.D. Irish and S.R. Douglas, "Validation of WIMS-IST", Proceedings of the 23rd Annual Conference of the Canadian Nuclear Society, Toronto, Ontario, Canada, 2002 June 2-5.

[3] J. Hu, I. Martchouk, R. Robinson, M. Ovanes and A. Buijs, "Simulation of Three-Dimensional Loss-of-Regulation Transients in ACR-1000 Reactors", Proceedings of the23rd Nuclear Simulation Symposium, "The Next Generation of Simulation Tools", Ottawa Marriott, Ottawa, Ontario, Canada, 2008 November 2-4.

[4] G. G. Chassie, Q. Jiang, H. Liu, M. Tochaie, and Z. Xu, "ELESTRES 2.1 Computer Code for High Burnup CANDU Fuel Performance Analysis" Proceedings of the 11th International Conference on CANDU Fuel, Niagra Falls, Ontario, Canada, 2010 October 17-20.